THEORIES OF HEATING OF SOLAR AND STELLAR CHROMOSPHERES

P. Ulmschneider

Institut für Theoretische Astrophysik,
Im Neuenheimer Feld 294,
D-6900 Heidelberg
Federal Republic of Germany, formerly

Institut für Astronomie und Astrophysik,
Am Hubland,
D-8700 Würzburg
Federal Republic of Germany

ABSTRACT. In the outer atmosphere of stars a rise of the kinetic temperature to values above T_{eff} is possible only if a large and persistent amount of mechanical heating is present. Constraints derived from empirical chromosphere models allow selection of important heating mechanisms from among a great number of possible processes. It appears that for non-magnetic regions short period acoustic waves and for magnetic regions Alfvén and slow mode magnetohydrodynamic waves are the dominant mechanisms. For non-magnetic cases new acoustic energy generation rates are reported. Non-magnetic theoretical chromosphere models for the sun and 10 other stars are discussed and compared with observations. Chromospheric heating in early type stars is briefly mentioned.

1. ENERGY BALANCE IN STELLAR CHROMOSPHERES

When in 1941 Edlén conclusively demonstrated that the mysterious solar coronal lines were produced by extremely highly ionized metals a firmly established astrophysical world had been shattered. The quarter century before Edlén, due to the work of Bohr, Saha, Milne, Eddington and others had seen the very successful explanation of stellar spectra based on the principle of radiative equilibrium introduced by Schwarzschild. This principle states that in the outer atmosphere of stars energy is exclusively transported by radiation. Applications before Edlén

R. M. Bonnet and A. K. Dupree (eds.), Solar Phenomena in Stars and Stellar Systems, 239–263.

however had shown that radiative equilibrium invariably lead to an outwardly decreasing temperature distribution which now was in obvious contradiction to Edlén's discovery of an extremely hot corona.

In recent years stellar observations of X-ray emission, of UV lines from highly ionized atoms, of Fe II emission lines and of the He 10830 Å line have indicated that the hot shell found in the case of the sun is for stars not an exception but rather a rule (32, 33, 45, 47). Let us define a hot shell as the stellar layer adjacent to the photosphere where the temperature increases outwardly to values higher than T_{eff}. Fig. 1 shows our present state of knowledge of the existence of hot shells around stars. It is seen that very likely all stars have hot shells. The inner parts of hot shells are called chromospheres.

Consider a gas element in a stellar chromosphere. If an amount of heat dQ enters this element the change of entropy S per gram is

$$dS = \frac{dQ}{\rho T} . \qquad (1)$$

Here ρ is the density and T the kinetic temperature. The entropy

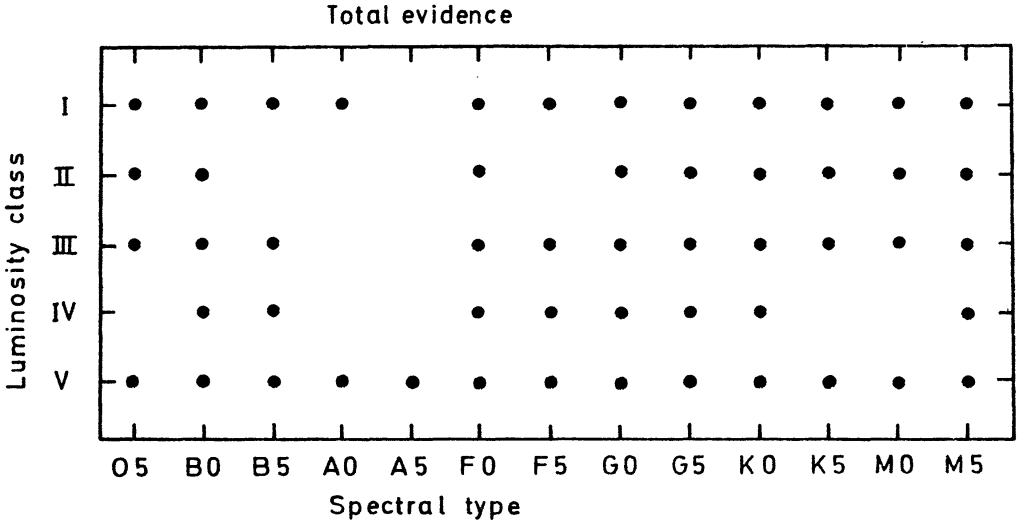

Figure 1. Stellar types (dots) where hot shells have been detected

or energy conservation equation valid for stellar chromospheres can be written

$$\frac{\partial S}{\partial t} + u \frac{\partial S}{\partial x} = \left.\frac{dS}{dt}\right|_{Rad} + \left.\frac{dS}{dt}\right|_{Visc} + \left.\frac{dS}{dt}\right|_{Cond} + \left.\frac{dS}{dt}\right|_{Mech} \qquad (2)$$

where x is the geometrical height, t the time and u the stellar wind velocity. The right hand side of equ. (2) represents the entropy gain due to radiative-, viscous-, conductive- and mechanical (that is acoustic or magnetic) heating originating from outside the gas element. For the solar chromosphere the time dependence and the influence of the stellar wind can be neglected and the left hand side of equ. (2) is zero. Furthermore in the low and middle chromosphere viscous heating and thermal conduction are very small (42). Thus the energy balance is mainly between radiative cooling and mechanical heating.

In a grey atmosphere for instance the gas element gains entropy by absorption of photons proportional to the mean intensity J but at the same time looses photons proportional to the integrated Planck function B

$$B = \frac{\sigma}{\pi} T^4 \ . \qquad (3)$$

We thus have

$$0 = \frac{4\pi\kappa(J-B)}{T} + \left.\frac{dS}{dt}\right|_{Mech} \qquad (4)$$

Here κ is the opacity per gram and σ the Stefan-Boltzmann constant. The sun at chromospheric heights can be crudely considered as a black body with an effective temperature T_{eff}. Because photons radiate only into one half space the mean intensity can roughly be written

$$J = \frac{1}{2} \frac{\sigma}{\pi} T_{eff}^4 \ . \qquad (5)$$

In absence of mechanical heating, that is in radiative equilibrium, it is seen from equ's (3) to (5) that the temperature decreases to a boundary temperature of

$$T = \sqrt[4]{\frac{1}{2}} T_{eff} \simeq 0.8 \ T_{eff} \qquad (6)$$

which for the sun (T_{eff} = 5770 K) is about 4900 K. This was the state before Edlén.

The observed large temperature increase with $T >> T_{eff}$ in the stellar chromospheres thus signifies after equ. (4) that in order to satisfy energy conservation a large and persistent amount of mechanical heating is necessary to hold the atmospheres in a steady state configuration. If this mechanical heating were switched off radiative equilibrium would be quickly reestablished. The time constant for reestablishment of radiative equilibrium is the radiative relaxation time

$$t_R = \frac{C_v}{16\kappa\sigma T^3} \tag{7}$$

where C_v is the specific heat per gram. Note that t_R for the solar chromosphere is in the range of minutes.

2. POSSIBLE CHROMOSPHERIC HEATING MECHANISMS

What mechanisms are responsible for the heating of stellar chromospheres? Clearly there are a great number of possible mechanisms which however are not all equally important. Moreover their importance may vary greatly from point to point in the atmosphere. Chromospheres are differentiated e.g. into dense and thin regions, into regions of large and small magnetic field strength, into regions of plane and very special magnetic field geometries. It presently appears that the chromospheric heating mechanisms can be grouped into three radically different types; explosive heating, quasisteady heating and wave heating (45).

The prototypes of the explosive mechanisms are those that generate flares which however occur rather infrequently and in special magnetic configurations. Somewhat more steady types of explosive mechanisms could be those that give rise to microflares, spicules and to the high velocity jets recently discovered by Brückner et al. (8). Aside from direct heating these mechanisms could bring considerable amounts of mass into the corona from where it is observed to flow back into the chromospheric network contributing to the enhanced emission.

A typical example of the second type, the quasi-steady heating mechanisms is the one recently proposed by Rosner et al. (37) for solar active regions. Here magnetic field tubes are twisted by the differential rotation of the sun. This twisting is relaxed by anomalous current dissipation that heats the flux tube. Note that the Rosner et al. mechanism has recently been criticized by Kuperus, Ionson and Spicer (28). Another mechanism of this type is the one of Somov and Syrovatskii (39). These

authors suppose that the formation of active regions is accompanied by the development of quasi-steady current sheets where magnetic field reconnection takes place. Both the explosive and quasi-steady mechanisms are strongly correlated with the magnetic field.

A third type of chromospheric heating mechanism is wave heating. A rich spectrum of different types of waves has been observed on the sun owing its existence to the four principal restoring forces. Pressure gives rise to acoustic waves, buoyancy to both internal gravity waves and convection, magnetic tension to Alfvén waves, coriolis forces to Rossby waves. Simultaneous action of more than two restoring forces produces additional wave forms like e.g. the fast and slow mode magnetohydrodynamic waves.

The long period acoustic modes have recently been reviewed by Deubner (15). Typical energy fluxes in the 160.0 min oscillation of Kotov et al. (27) are less than $2 \cdot 10^3$ erg/cm^2 s at the base of the photosphere if these waves were propagating. Presently however it is still debated whether these modes actually exist. The 5 min oscillations are an outstanding well observed phenomenon on the sun with amplitudes of the order of 500 m/s. Observations however show (13) that these acoustic modes are largely standing waves with a phase shift of about 90° between velocity and brightness fluctuations. Canfield and Musman (10) find for these waves an energy flux of $8 \cdot 10^5$ erg/cm^2 s at 490 km height and of $2 \cdot 10^4$ erg/cm^2 s at 1000 km.

Short period waves with periods from a few seconds to minutes have been detected by Deubner (14) using lines of C, Fe and Na in the visible. As these waves have periods less than the acoustic cut-off period of about 180 s they will propagate and transport energy. Deubner finds a short period acoustic flux of between 10^8 and 10^9 erg cm^{-2} s^{-1} which probably is an upper estimate. This flux value has been discussed by Cram (11) and criticized by Durrant (16). Independently Stein (40) has found theoretically a short period acoustic flux of between $7 \cdot 10^6$ and 10^8 erg/cm^2 s with a frequency spectrum that peaks considerably above the acoustic cut-off frequency (ω_1 = .034 Hz) of the temperature minimum. In observations of Si II lines with the OSO-8 satellite in the upper chromosphere Athay and White (2) obtain a flux of only 10^4 erg cm^{-2} s^{-1}. Because of the low resolution of OSO-8 this probably is an underestimate. As the resolution of the OSO-8 spectrometer used for the Si II observations is 20 arc sec the measurements from this instrument could very likely lead to serve horizontal averaging. In addition the wavelength of short period acoustic waves is usually small compared to the width of the contribution function of the spectral line which results in vertical averaging. Both difficulties were recognized by Athay and White. Thus presently the magnitude of the observed short period acoustic

flux is uncertain by a considerable margin even if one takes into account that most of this flux would be dissipated at the height of Si II formation. Note however, that short period acoustic wave energy is clearly seen in Lyα observations of Artzner et al. (1) from OSO-8 and also in radio observations by Butz, Hirth and Fürst (9).

Just recently Brown and Harrison (7) have observed gravity waves on the sun. These waves so far were difficult to detect because they cannot exist in the unstable convection zone and are strongly damped in the radiative damping zone at heights of less than 100 km. Convection the unstable version of gravity waves on the other hand is easily seen as granulation. Here the overshooting of fast rising convective elements will give rise to acoustic waves which however are already included in the above mentioned short period wave observations.

Although magnetohydrodynamic waves must exist on the sun they have so far not been detected except for Alfvén waves above sunspots (5). Recently Stein and Leibacher (43) as well as Stein (41) have computed Alfvén wave fluxes of between 10^8 and $3 \cdot 10^9$ erg/cm^2 s from strong field regions. The reason why such large fluxes have not been observed probably lies in the fact that Alfvén waves are transverse waves with small variations of the gas pressure. Most of the Alfvén wave flux is reflected by the transition layer while an average flux of about $3 \cdot 10^5$ erg/cm^2 s is transmitted into the corona. Alfvén surface waves are proposed as heating mechanism for coronal loops (24). Stein (41) has computed a flux of slow mode mhd waves which is of the same order of magnitude as the Alfvén wave flux due to monopol sound generation in both cases. He finds that the fast mode mhd flux however is much smaller. Yet fast mode mhd waves have been proposed as heating mechanism for coronal loops (20). Finally the horizontally propagating Rossby waves have large periods and appear to carry little energy.

3. EVIDENCE FROM EMPIRICAL MODELS

What parameters can be derived from empirical chromosphere models that allow a selection among the many possible heating mechanisms? The most accurate and elaborate stellar chromosphere models are those for the sun by Vernazza, Avrett, Loeser (48) henceforth called VAL 80. These models are based on a wealth of visible UV, infrared, line and continuum data. VAL 80 have presented a series of models valid for a broad range of solar regions from a dark inner cell point to a very bright network element. In spite of the fact that these models are very sophisticated in that they carry out detailed solutions of the hydrostatic, radiative transfer and statistical equations for a great number of lines and

continua, they suffer from a possibly dangerous restriction. They largely neglect the dynamical nature of the atmosphere. The VAL 80 models include dynamical effects only in form of a microturbulence distribution and assume a smooth temperature profile. Here the presence e.g. of large amplitude acoustic waves, through the nonlinearity of the Planck function and the velocity-temperature correlation in the wave, may generate important effects (12).

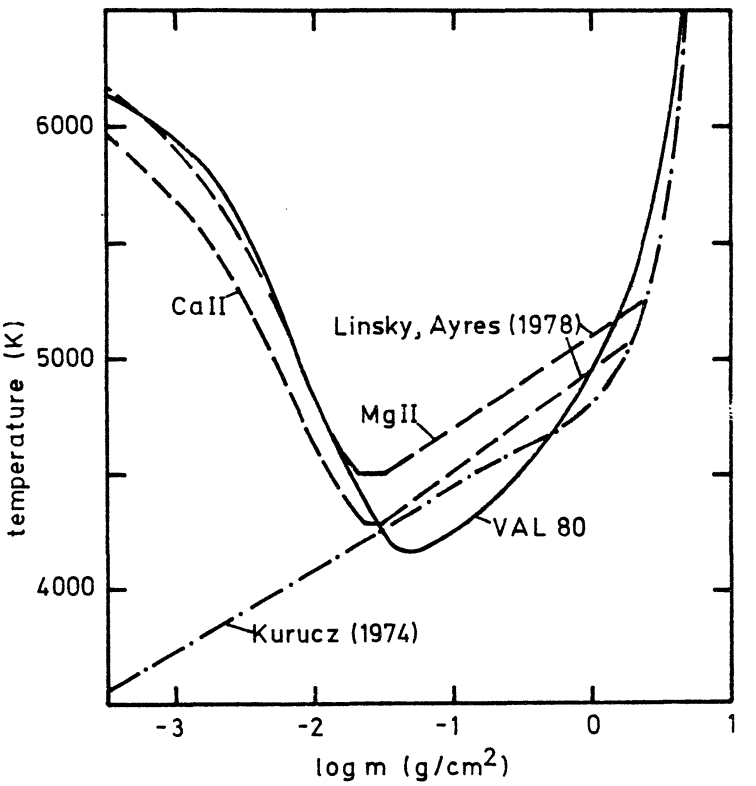

Figure 2. Empirical solar atmosphere models

Using information only from line profiles mainly of Ca II and Mg II but also of Si II, Si III, C II empirical chromosphere models for a considerable number of stars have been constructed (see reviews 32, 33, 45). For stars other than the sun such models are presently the only available chromosphere models. Fig. 2 shows for the sun a comparison of Ca II and Mg II line models of Linsky and Ayres (34) with the VAL 80 average sun model and a theoretical LTE radiative equilibrium model of Kurucz (29). There are systematic differences between these models. The Mg II model is hotter than the Ca II model and in the photosphere both line models are hotter than the VAL 80 model. This may be partly

due to a different weight given to the bright network areas by the line models. On the other hand dynamical effects also explain part of this discrepancy. The empirical VAL 80 model in the temperature minimum area is much cooler than the theoretical model. As non-LTE effects (Cayrel mechanism) are expected to further raise the theoretical temperature it seems highly likely that this discrepancy is due to the dynamical nature of the atmosphere as discussed below.

Keeping in mind these uncertainties in the empirical chromosphere models we now list parameters which may be useful for the selection of heating mechanisms.

I. The total chromospheric radiation loss F_E

As the existence of chromospheres is directly linked to the availability of mechanical energy the total chromospheric radiation loss F_E is in principle the most powerful selection criterion. The difficulty here is that this parameter is not easily evaluated from empirical models. E.g. considerable controversy exists in the literature as to whether H^- loss is a dominant contribution or not (3, 25, 35, VAL 80). Here the difficulties are the importance of non-LTE effects and how to separate the chromospheric loss from the photospheric radiative equilibrium loss. A similar, however much less severe situation exists for the Ca II losses, $F_{Ca\ II}$. Only the chromospheric Mg II losses, $F_{Mg\ II}$, due to the low photospheric contribution can be measured relatively unambiguously. However, the Mg II losses represent only about 20 percent of the total losses and this percentage varies from star to star (34).

II. The height of the temperature minimum m_T

Both in empirical models (VAL 80, Fig. 49) and in theoretical models (38) the temperature minimum coincides closely with a height where the mechanical dissipation increases rapidly with altitude. This height is usually measured either on a geometrical x_T or on a mass column density scale m_T. Because purely radiative means exist that raise the kinetic temperature in an atmosphere (Cayrel mechanism) the energy balance at the temperature minimum region in empirical models has to be closely checked.

III. The steepness of the chromospheric temperature rise dT/dm

The steepness of the chromospheric temperature rise depends sensitively on the distribution of both mechanical dissipation and radiative loss rates in the atmosphere.

IV. The variation of F_E, $F_{Ca\ II}$, $F_{Mg\ II}$, m_T, dT/dm with magnetic field strength $\vec{B}$

The empirical VAL 80 models of magnetic and nonmagnetic regions show characteristic differences. While the total flux F_E appears strongly affected, the temperature minimum heights m_T are not much changed. This is also observed for stars other than the sun. Due to a different coverage by plage areas of stars of similar T_{eff} and gravity the total Ca II and Mg II emission $F_{Ca\ II}$, $F_{Mg\ II}$ can vary by a factor of ten (4). On the other hand the Wilson-Bappu-effect which concerns the width of the Ca II emission core and thus the height of the temperature minimum does not show a great age or magnetic field dependence (17).

V. The variation of F_E, $F_{Ca\ II}$, $F_{Mg\ II}$, m_T, dT/dm with T_{eff}, gravity and average field strength $\bar{B}$

The systematic variation of the chromospheric parameters F_E, $F_{Ca\ II}$, $F_{Mg\ II}$, m_T or dT/dm with T_{eff} and gravity is a powerful selection criterion which for chromospheric heating mechanisms is useful even if the absolute magnitude of the produced heating flux is uncertain. For example see Stein (41), and the acoustic heating results below.

4. ACOUSTIC HEATING AS THE DOMINANT MECHANISM FOR THE LOW CHROMOSPHERE

On basis of the data available from empirical chromosphere models we now try to identify important heating mechanisms for stellar chromospheres. In Tab. 1 total chromospheric and coronal radiation losses given by various authors and summarized by Ulmschneider (45) are compared with recent determinations from VAL 80. Values in brackets are taken from (45). In spite of considerable disagreements due to differing views on the H^- losses and the Ca II IRT the total losses do not appear to be greatly in dispute: A solar chromospheric heating mechanism should provide a mechanical flux of about $F_E = 6 \cdot 10^6$ erg/cm^2 s at the base of the chromosphere.

From this flux value it is immediately obvious that from the wave mechanisms the long period modes are excluded. The same can be said about the 5 min oscillations. These waves can be excluded also on other grounds. The long wavelengths of the 5 min oscillations preclude any appreciable viscous or conductive heating. Radiative damping as a heating mechanism by these waves is effective only in the lower photosphere. Thus shock dissipation remains as the only potential heating mechanism. Shock dissipation is however excluded for the 5 min oscillations because of the observed 90° phase shift. It is a general property of shock waves

Table 1. Chromospheric radiative loss rates

Source	Ulmschneider (1979) loss [erg/cm^{2}s]	VAL 80 loss [erg/cm^{2}s]
H^-	$30 \cdot 10^5$	$4 \cdot 10^5$
Ca II	$8 \cdot 10^5$	$30 \cdot 10^5$
Mg II	$10 \cdot 10^5$	$9 \cdot 10^5$
H_α	$5 \cdot 10^5$	-
Mg I, Na I, Ca I, Fe I, Fe II, etc.	$4 \cdot 10^5$	$(4 \cdot 10^5)$
$L\alpha$	$2 \cdot 10^5$	$3 \cdot 10^5$
Corona and transition layer	$3 \cdot 10^5$	$(3 \cdot 10^5)$
	$62 \cdot 10^5$	$53 \cdot 10^5$

that velocity and temperature shock simultaneously producing a 0^o phase shift. Thus the 5 min oscillation cannot produce a temperature minimum at the observed height.

The explosive and quasi-steady mechanisms primarily apply to the upper chromosphere and the corona where magnetic effects dominate. For the lower and middle chromosphere where most of the chromospheric energy loss originates these mechanisms do not apply because of the energy requirement. Tab. 1 shows that the averaged energy requirements for coronal loops are by an order of magnitude smaller than for the chromosphere.

Thus the only remaining powerful heating mechanisms are short period acoustic waves and magnetohydrodynamic waves. In spite of the observational uncertainty it appears that the energy requirement of $F_E = 6 \cdot 10^6$ erg/cm^2 s is met for short period acoustic waves. In addition, these waves as shown below, are able to produce the temperature minimum at the observed height. In network areas calculations of Stein and Leibacher (43) as well as Stein (41) show that Alfvén and slow mode mhd waves are both efficiently produced. The magnitude of this mhd wave flux appears sufficient but is still rather uncertain. A detailed study is missing. Alfvén waves are difficult to dissipate in the chromosphere (44), but surface waves in the presence of strong gradients of the Alfvén velocity are thought to dissipate significantly (24). Yet it seems difficult for Alfvén waves to explain the

height of the temperature minimum. Here the slow mode waves are an attractive companion/alternative. Slow mode waves in regions of strong magnetic fields are essentially acoustic waves that propagate along the magnetic field lines. They would be seen as acoustic waves, being included in Deubners (14) observations. They could form shocks at the temperature minimum area and through their magnetic nature would explain the variability of the stellar Mg II and Ca II emission. Moreover Stein (41) has shown that both slow mode and Alfvén waves can explain the missing gravity dependence of the stellar Mg II emission.

At this point an important fact should be noted. If the computation of the empirical chromospheric radiation flux is not grossly in error the chromosphere cannot accept more energy than F_E. Thus any mechanism which provides F_E must be the dominant one and the other mechanisms should be found to be considerably less energetic. We thus conclude that for nonmagnetic regions the short period acoustic waves very likely are the dominant mechanism while for network areas with strong magnetic fields Alfvén and slow mode waves appear as the main mechanical input for the low and middle chromosphere. Here the acoustic-like slow mode waves seem to be especially important for producing - through the onset of shock dissipation - the required rapidly increasing mechanical heating at the temperature minimum area $x \geq x_T$.

5. ACOUSTIC ENERGY GENERATION

For the generation of non-magnetic acoustic waves a fairly well developed theory exists (31, 40) while for the production of magnetohydrodynamic waves only rough estimates (41, 43) are presently available.

The acoustic energy generation in stars is calculated in two steps. For a star of given T_{eff} and gravity one first constructs a convection zone model where for the mixing length theory one in addition needs the parameter $\alpha = \ell/H$, the ratio of mixing length to pressure scale height. Then Lighthills (31) theory is applied. In its simplest form this latter theory neglects magnetic fields as well as gravity and considers a homogeneous atmospheric layer with density ρ_0 and pressure p_0 as well as a localized field of turbulent velocities $\vec{v}$. The turbulent field generates small density ρ', pressure p' and velocity $\vec{u}$ perturbations. In the turbulent field $|\vec{v}|$ is not assumed small but $|\vec{u}| << |\vec{v}|$. One has

$$\frac{\partial \rho'}{\partial t} + \frac{\partial \rho v_i}{\partial x_i} = 0 \qquad (8)$$

$$\frac{\partial \rho v_i}{\partial t} + \frac{\partial \rho v_i v_j}{\partial x_j} + \frac{\partial p'}{\partial x_i} = 0 \tag{9}$$

$$p' = c_o^2 \rho' \tag{10}$$

where c_o = const is the sound velocity. From these equations a wave equation is found

$$(\nabla^2 - \frac{1}{c_o^2}\frac{\partial^2}{\partial t^2})\rho' = -\frac{1}{c_o^2}\frac{\partial^2 \rho_o v_i v_j}{\partial x_i \partial x_j} \tag{11}$$

with a quadrupole source term which can be solved for large distances $|\vec{x}| >> |\vec{x}'|$ from the turbulent field

$$\rho' \simeq \frac{\rho_o}{4\pi c_o^4}\frac{x_i x_j}{|\vec{x}|^3}\int \frac{\partial^2}{\partial t^2} v_i v_j d^3x'. \tag{12}$$

With the relation $u = \rho' c_o/\rho_o$ valid for acoustic waves the acoustic flux is the time average

$$F_M = \overline{p'u} = \frac{c_o^3}{\rho_o}\overline{\rho'^2} = \frac{\rho_o}{4\pi c_o^5}\frac{x_i x_j x_k x_\ell}{|\vec{x}|^6}\iint \overline{\frac{\partial^2}{\partial t^2} v_i v_j \frac{\partial^2}{\partial t^2} v_k v_\ell} d^3x' d^3x'' \tag{13}$$

For the turbulent velocities assumptions must be made on the spacial and temporal correlations $v(\vec{x}',t')v(\vec{x}'',t'')$. These assumptions together with the mean turbulent velocity v from the convection zone model allow evaluation of equ. (13),

$$F_M = \int 38 \frac{\rho_o v^8}{c_o^5 \ell}\, dx \tag{14}$$

Fig. 3 shows (drawn) the acoustic energy flux F_M computed this way by Renzini et al. (36). It is seen that F_M rises rapidly with increasing T_{eff} and decreasing gravity. As the convection zones become inefficient for early type stars, F_M abruptly decreases at high T_{eff}.

Newest UV and X-ray observations indicate however that especially for late type dwarf stars the homogeneous atmosphere assumption in Lighthills theory breaks down. Recent work of Bohn (6) following Stein (40) aside of improving the treatment of H_2 molecules includes gravity in Lighthills theory. Stein (40) has shown that then the source term at the right hand side of equ. (11) is essentially replaced by

$$A \frac{\partial^2 \rho_o \overline{2v_i v_j}}{\partial x_i \partial x_j} + B \frac{\omega_1}{c_o} \frac{\partial \rho_o \overline{2v_j v_z}}{\partial x_j} + C \frac{\omega_1^2}{c_o^2} \rho_o \overline{2} \, v_z v_z \qquad (15)$$

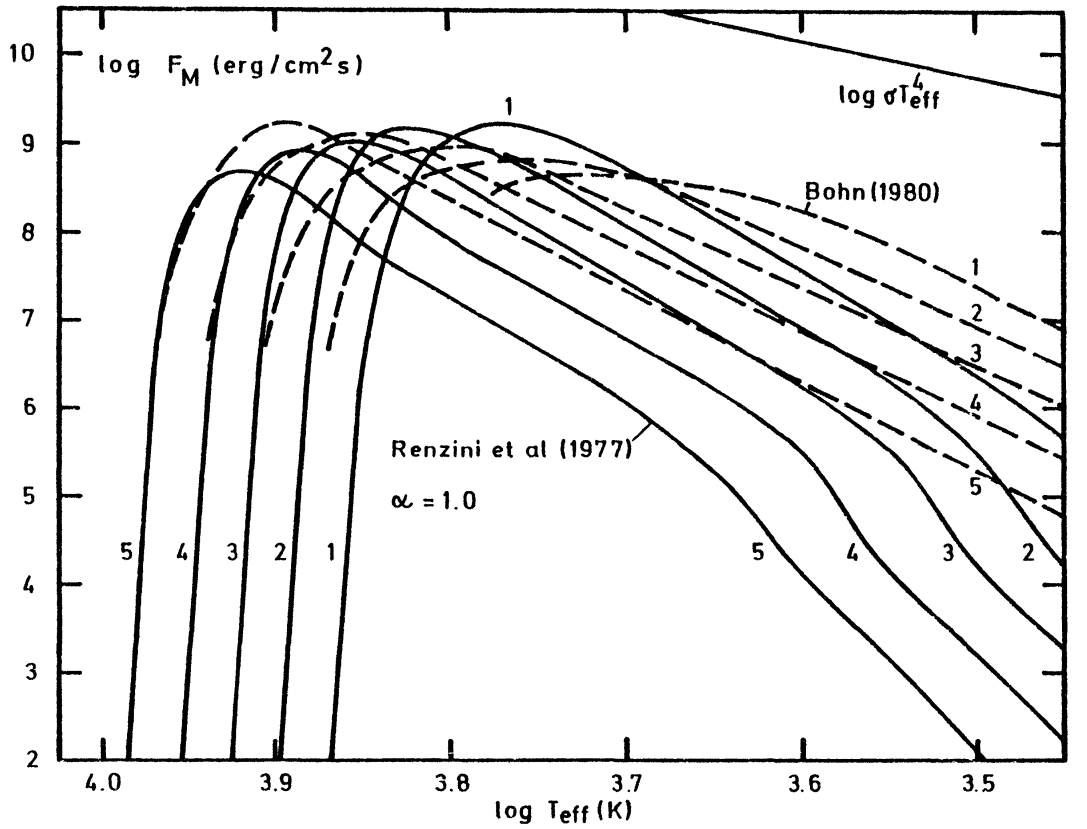

Figure 3. Non-magnetic acoustic energy generation rates as function of T_{eff} with log g as parameter

where z is the vertical direction, ω_1 the acoustic cut-off frequency and A, B, C constants. Bohn finds that especially towards late type dwarf stars the much more efficient dipole and monopole source terms in equ. (15) dominate as is shown in Fig. 3 (dashed). For late type stars the acoustic flux is there considerably magnified.

As shown by Stein and Leibacher (43) and Stein (41) the inclusion of strong magnetic fields modifies equ's (9), (10) still

further leading to monopole source terms for Alfvén and slow mode waves as well as to quadrupole terms for fast mode waves. These fluxes considerably further enhance Bohn's (6) values in strong magnetic field areas.

In addition to the total wave flux F_M, Stein (40) and Bohn (6) also give the monochromatic flux $dF_M/d\nu$. The peak of this flux spectrum is for the sun roughly at the frequency

$$\nu_{Max} = \frac{1}{P_{Max}} \simeq \frac{10}{2\pi}\omega_1 = \frac{10}{4\pi}\frac{\gamma g}{c} \simeq \frac{c}{H} \qquad (16)$$

where γ is the ratio of specific heats. From a peak given by equ. (16) the acoustic spectrum falls off to both larger and smaller frequency. The decay towards larger frequency is produced by the decrease of velocity with frequency in the turbulence spectrum. Here different assumed turbulence spectra (Kolomogoroff, Spiegel or exponential (40)), give different decays of the acoustic flux with frequency. Towards lower frequency the decrease of the flux is due to the acoustic cut-off frequency which decreases with increasing temperature.

6. THEORETICAL SOLAR CHROMOSPHERE MODELS

For a given type of star and given magnetic field structure theoretical chromosphere models can be constructed in principle by solving the magnetohydrodynamic equations and the radiative transfer equation. At the present time this procedure has been carried out only for non-magnetic cases and only for rather simplified circumstances. The specification of two parameters T_{eff} and gravity allows to compute the acoustic flux F_M as shown above. The third parameter α is usually thought to vary only within the narrow limits α = 1.0 to 1.5 (19). A comparison of recent radial and nonradial pulsation calculations with observed solar 5 min oscillations does not disagree with this view (38). Thus for non-magnetic cases essentially a two parameter set of theoretical chromosphere models is obtained.

In the most recent calculations summarized by Ulmschneider (45) a series of severe simplifications are made. Instead of a spherically propagating acoustic spectrum one assumes a plane monochromatic wave with frequency ν_{Max} and neglects effects due to ionization. The radiation transport is evaluated with a grey LTE two-stream approximation.

Consider a plane stellar atmosphere bounded below by a piston and at the top by a transmitting, fluid type boundary. Within this slab shockfronts act as internal boundaries separating

continuous regions. For these regions the hydrodynamic equations can be written

$$\frac{\partial \rho}{\partial t} + \frac{\partial \rho u}{\partial x} = 0 \tag{17}$$

$$\rho \frac{\partial u}{\partial t} + \rho u \frac{\partial u}{\partial x} + \frac{\partial p}{\partial x} + \rho g = 0 \tag{18}$$

$$\frac{\partial S}{\partial t} + u \frac{\partial S}{\partial x} = \left.\frac{dS}{dt}\right|_{Rad} \tag{19}$$

while the Hugoniot relations connect across the shocks. With the equations

$$p = \rho \frac{\mathcal{R} T}{\mu}, \quad \rho = \rho_o \left(\frac{T_o}{T}\right)^{3/2} e^{-\frac{(S-S_o)}{\mathcal{R}}\mu}, \quad c^2 = \gamma \frac{\mathcal{R} T}{\mu} \tag{20}$$

valid for neutral ideal gases where $\mathcal{R}$ is the gas constant and c the sound velocity, three of the five thermodynamic variables p, ρ, T, c, S can be eliminated. ρ_o, T_o, S_o refer to the undisturbed atmosphere. The radiative transfer equation is solved in the LTE two stream approximation

$$\pm \frac{1}{\sqrt{3}} \frac{dI^{\pm}}{dx} = -\kappa\rho(I^{\pm} - B) \tag{21}$$

where

$$J = \frac{I^{+} + I^{-}}{2}, \quad B = \frac{\sigma}{\pi} T^4 \tag{22}$$

and with equ. (4)

$$\left.\frac{dS}{dt}\right|_{Rad} = \frac{4\pi\kappa}{T}(J - B). \tag{23}$$

Here κ is the grey opacity per gram and $I^{\pm}$ the specific intensity. The boundary conditions are:

$$\text{at the piston: } u = -\sqrt{\frac{2F_M}{\rho c}} \sin(2\pi\nu_{Max} t), \quad I^{+} = \frac{\sigma}{\pi} T^4 + \frac{\sqrt{3}\sigma}{4\pi} T_{eff}^{\ 4} \tag{24}$$

at the top: $u = u(x-(c+u)\Delta t,\ t-\Delta t),\ \bar{I} = 0.$ (25)

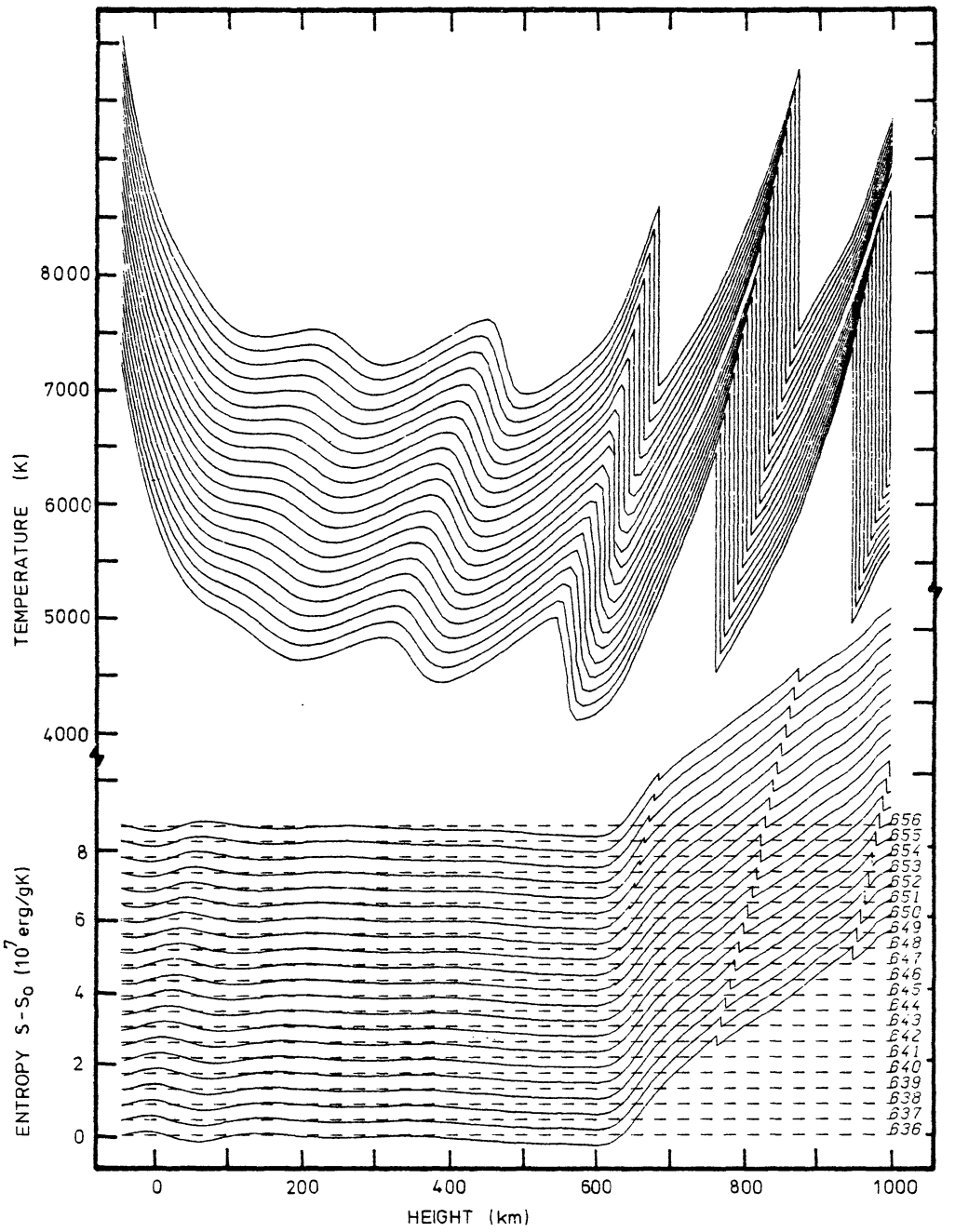

Figure 4. Temperature and entropy as function of height. Successive time steps (Δt = 0.95 s) are displaced for clarity. Scales are for the lowest curves

Starting initially with a radiative equilibrium atmosphere labeled T_{RE} in Fig. 5 the temperature and entropy distributions after some time are shown in Fig. 4. Roughly after 20 shocks have been transmitted at the top boundary the mean time averaged quantities approach a steady state. Fig. 5 shows a comparison of thus obtained theoretical chromosphere models (drawn) with empirical models (dashed) for the sun (46). The range of α indicates the remaining freedom of choice for the theoretical models. Relatively good agreement is seen for both the height of the temperature minimum and the chromospheric temperature gradient.

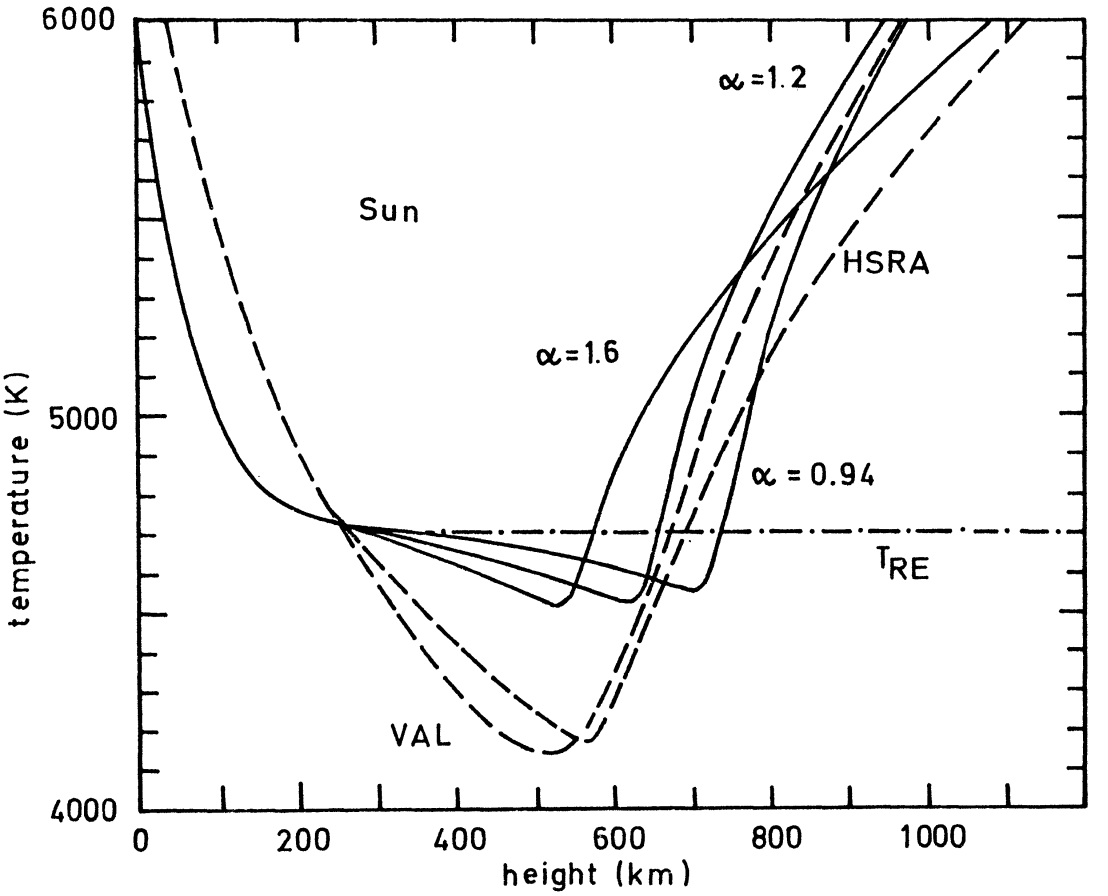

Figure 5. Time averaged theoretical and empirical solar models

A rather unexpected feature of the theoretical models (c.f. Fig. 5) is the photospheric temperature depression below the radiative equilibrium distribution T_{RE}. This is due to the large amplitude of the acoustic waves and the nonlinearity of the Planck

function. As in steady state the time averaged mechanical dissipation must be equal to the averaged radiation loss we have from equ. (4)

$$\overline{\frac{dF_M}{dx}} = 4\pi\kappa\rho(\overline{J-B}). \qquad (26)$$

In the upper photosphere a negligible amount of radiation damping leads to $dF_M/dx \simeq 0$. The mean intensity J originating from optical depth $\tau \simeq 1$ where acoustic waves have small amplitude is essentially constant. Thus roughly $J \simeq B$. But the phase $T^4 = (\bar{T} + \Delta T)^4$ of the wave contributes disproportionately much compared with the phase $T^4 = (\bar{T} - \Delta T)^4$ such that $\bar{T} < T_{RE}$. Note that this dynamical behaviour explains readily the observed temperature depression below Kurucz's (29) model (c.f. Fig. 2). The discrepancies between empirical and theoretical models in the photosphere (c.f. Fig. 5) are mainly due to the grey approximation used for the theoretical models as can be seen by comparing the T_{RE} distribution of Fig. 5 with Kurucz non-grey model in Fig. 2.

7. EMPIRICAL AND THEORETICAL CHROMOSPHERE MODELS OF LATE TYPE STARS

With the same methods as used for the sun theoretical chromosphere models of other stars can be constructed. Here likewise only models disregarding magnetic fields are presently available. The non-magnetic theoretical models are uniquely determined by specifying (in addition to the parameter α) only the two variables T_{eff} and gravity.

In Fig. 6 theoretical temperature minima for eleven late type stars are shown (triangles) together with temperature minima from semiempirical models (dots) based on Ca II line observations (38). The acoustic energies used for the computation of these theoretical chromosphere models are calculated in the approximation of Renzini et al. (36) and assuming $\alpha = 1.25$. A rather good agreement is seen except for late type dwarf stars where there is increasing discrepancy towards low T_{eff}. E.g. for 70 OphA a factor of five and for EQ Vir a factor of 145 more acoustic energy is needed to bring agreement between theory and observation. This discrepancy however is now largely eliminated due to Bohn's (6) new values of the acoustic flux (see Fig. 3). For the active chromosphere star EQ Vir a factor of about three remains even if Bohn's flux is taken into account. This discrepancy is very likely due to the neglect of magnetic fields in the computation of the acoustic energy generation of Fig. 3.

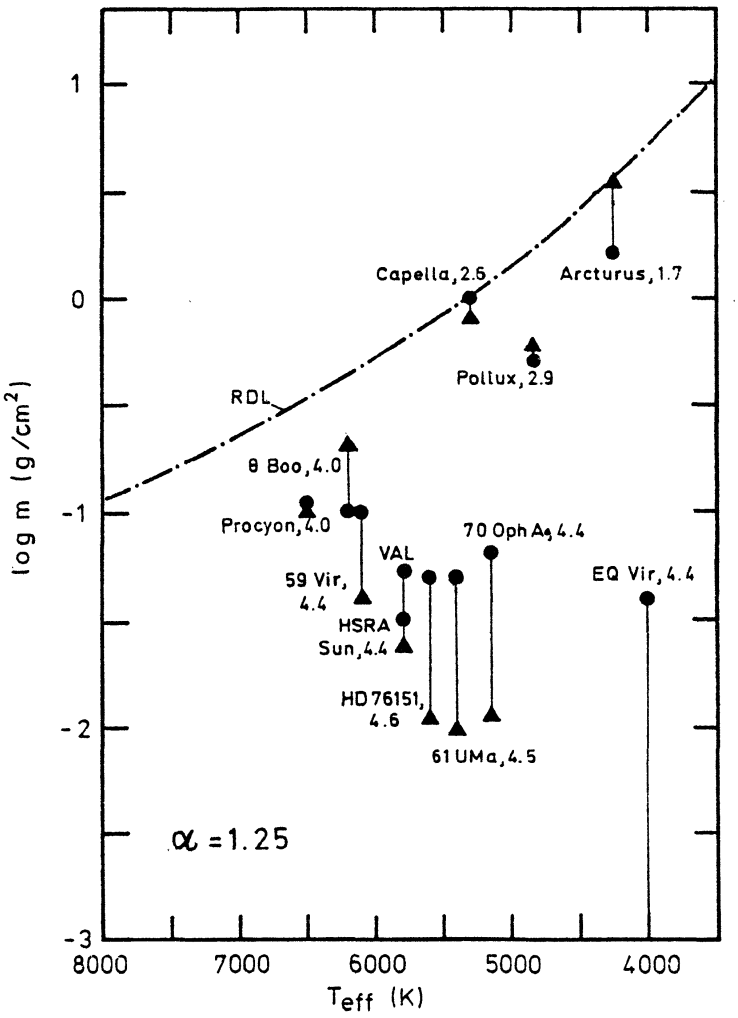

Figure 6. Theoretical and empirical heights of the temperature minimum for individual stars

Fig. 7 after Schmitz and Ulmschneider (38) shows theoretical mean temperature distributions for various stellar models identified by T_{eff} and log g. Here again $\alpha = 1.25$. These temperatures should be compared with semiempirical chromosphere models and chromospheric temperature gradients shown in Figs. (8) and (9) based on Ca II K line observations of Kelch, Linsky and Worden (26). As can be seen by comparing the theoretical models (T_{eff}, log g) = (4000 K, 2), (4000 K, 4) and (6000 K, 4) of Fig. 7 the chromospheric temperature gradient increases with increasing gravity and decreasing T_{eff} in agreement with the observations (Fig. 9).

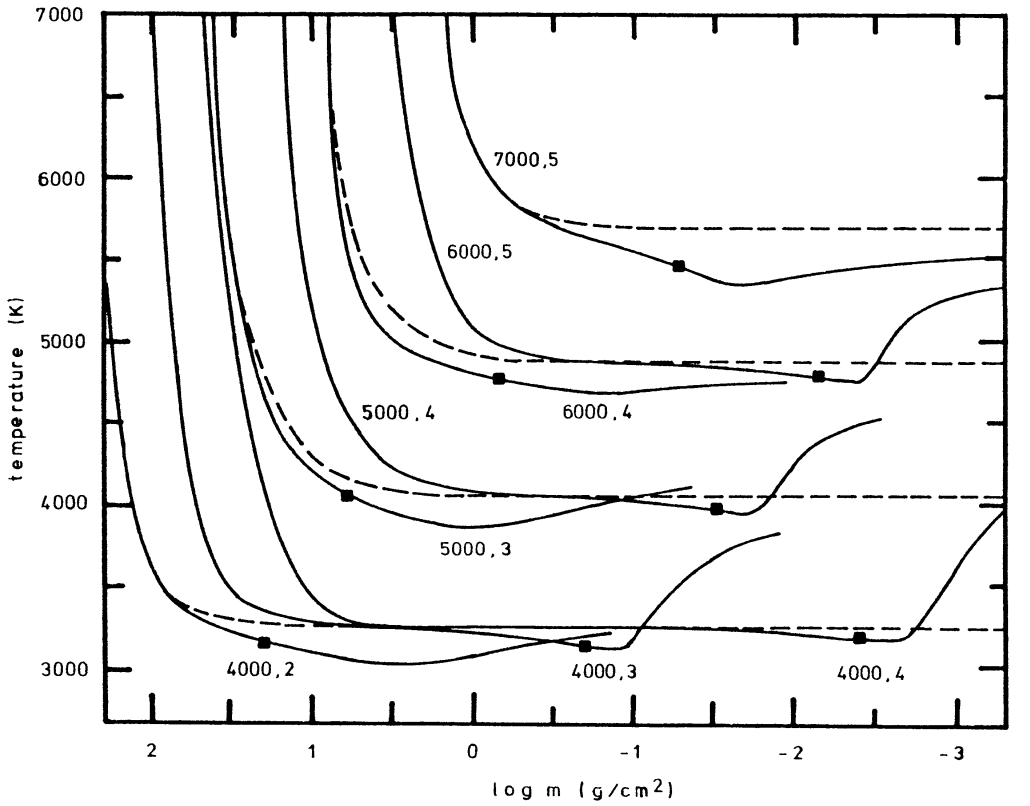

Figure 7. Time averaged theoretical atmosphere models for stars of indicated T_{eff} and log g. Radiative equilibrium models are shown dashed

A comparison of Fig. 7 and 8 (dashed) shows considerable differences in the temperature structure caused by the grey and non-grey approximations used in the theoretical and semiempirical models respectively. However even if non-grey radiative transport were taken into account in the theoretical models the fact that all these models show photospheric temperature depressions would not vanish as this is a consequence of the large amplitude of the waves and the nonlinearity of the Planck function as discussed for the solar case.

Interestingly however the empirical models invariably show photospheric temperature enhancements. In Fig. 7 filled squares show the height of shock formation. It is seen that for stars of large gravity and low T_{eff} the heights of shock formation are closely correlated with the temperature minimum positions. These chromosphere models have been called S-type chromospheres. Stars with high T_{eff} or low gravity have shock formation heights considerably different from the temperature minimum heights. Such stellar models have been called R-type chromospheres as there the process of radiation damping determines the position of the tempe-

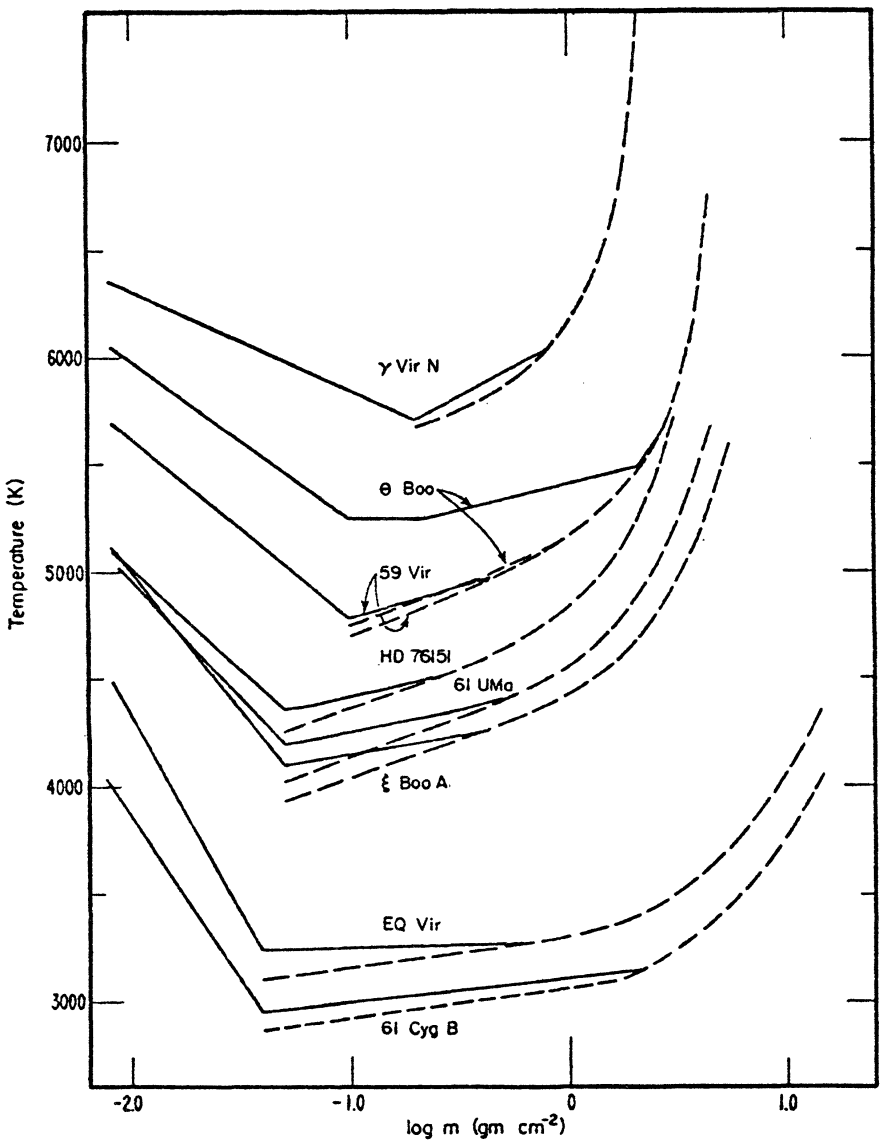

Figure 8. Empirical atmosphere models (Kelch, Linsky, Worden 1979)

rature minimum. R-type chromospheres have rather extensive photospheric temperature depressions. From their values of T_{eff} and g, stars like θBoo, αAur, αOri or αCMi should have R-type chromospheres. These stars are observed to have extensive photospheric temperature enhancements. The remaining stars of Fig. 8 are all S-type chromosphere stars and have small photospheric temperature enhancements. Thus theoretical computations and observations complement each other. Where an empirical model shows high tempe-

rature enhancement, the corresponding theoretical model shows large temperature depression. This behaviour has been explained (38) by the fact that the Planck function at the frequencies of

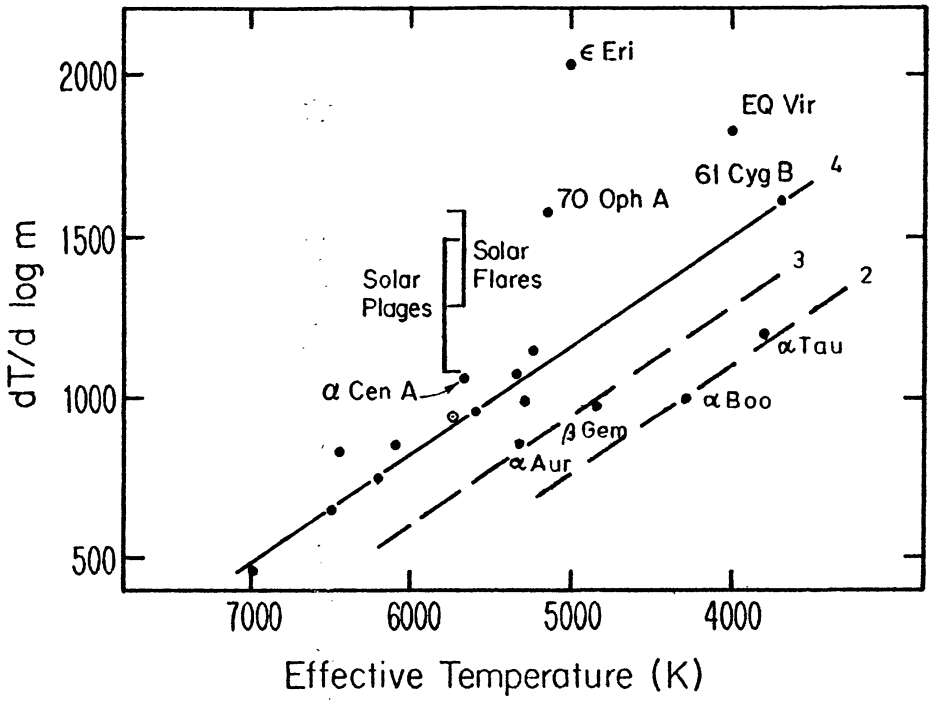

Figure 9. Empirical chromospheric temperature gradients for dwarf stars (Kelch, Linsky, Worden 1979) together with values for αAur, βGem, αBoo and αTau. Lines are labelled by log g

the Ca II K and Mg II h,k lines has a very steep temperature dependence such that only the wave crests of the large amplitude acoustic waves are seen at these UV frequencies. Thus the infered empirical models based on Ca II K are considerably hotter than the time averaged theoretical models. As in turn the temperature dependence for Mg II k (λ 2793 Å) is much larger than for Ca II K (3933 Å) we expect by the same effect the Mg II models to be much hotter than the Ca II models. This has actually been observed (c.f. Fig. 2).

As the chromospheric radiation flux F_E should be roughly equal to the acoustic energy at the temperature minimum F_{MT} if the acoustic mechanism is the dominant chromospheric heating mechanism these two quantities have been compared in previous work. Rough agreement has been found (38). As a considerable controversy has recently arisen in the literature about the importance of the H^- losses these comparisons of the acoustic flux and the total chromospheric losses do not carry much weight pre-

sently. Fig. 3 of Schmitz and Ulmschneider (38) shows the comparison of the acoustic flux at the temperature minimum of eleven stars with the average Mg II k emission flux given by Basri and Linsky (4). The acoustic fluxes also decrease with decreasing T_{eff} and are roughly a factor of ten above the Basri and Linsky line. This factor of ten agrees with the ratio of total to Mg II k line losses as given above by Tab. 1. It is clear that the variability of the Mg II k line emission in stars of similar T_{eff} and gravity cannot be explained by the present non-magnetic theoretical models. Here slow mode heating models will have to be constructed.

8. CHROMOSPHERIC HEATING IN EARLY TYPE STARS

The recent X-ray observations with the Einstein satellite (47) together with UV observations of O VI, N V and Si IV lines summarized by Ulmschneider (45) and in Fig. 1 conclusively demonstrate the existence of hot shells in early type stars. As these stars do not have efficient convection zones (c.f. Fig. 3) another wave energy generation mechanism must be at work. A very attractive possibility is that observed turbulent gas motions are amplified by the radiation field of the star. Hearn's (21, 22, 23) mechanism considers amplification of isothermal acoustic waves by the κ-mechanism. If primordial magnetic fields are present on early type stars slow mode waves could be amplified by the same process. Rough calculations for non-magnetic cases produce acoustic energies which are in relative good agreement with empirical values derived from photospheric turbulence (30). A detailed investigation is however missing at the present time.

REFERENCES

(1) Artzner, G., Leibacher, J., Vial, J.C., Lemaire, P., Gouttebroze, P.: 1978, Astrophys. J. 224, pp. 83-85.
(2) Athay, R.G., White, O.R.: 1978, Astrophys. J. 226, pp. 1135-1139.
(3) Ayres, T.R.: 1980 preprint.
(4) Basri, G.S., Linsky, J.L.: 1979, Astrophys. J. 234, pp. 1023-1035.
(5) Beckers, J.M.: 1976, Astrophys. J. 203, pp. 739-752.
(6) Bohn, H.U.: 1980, to be published.
(7) Brown, T.M., Harrison, R.L.: 1980, Astrophys. J. Letters, in press.
(8) Brückner, G.E., Bartoe, J.D.F., von Hoosier, M.E.: 1978, in E. Hansen and S. Schaffner eds., Proceedings OSO-8 workshop.
(9) Butz, M., Hirth, W., Fürst, E.: 1979, Astron. Astrophys. 72, pp. 211-214.

(10) Canfield, R.C., Musmann, S.: 1973, Astrophys. J. 184, pp. L131-L136.
(11) Cram, L.E.: 1977, Astron. Astrophys. 59, pp. 151-159.
(12) Cram, L.E., Keil, S.L., Ulmschneider, P.: 1979, Astrophys. J. 234, pp. 768-774.
(13) Deubner, F.: 1974, Solar Physics 39, pp. 31-48.
(14) Deubner, F.: 1976, Astron. Astrophys. 51, pp. 189-194.
(15) Deubner, F.: 1980, Highlights of astronomy 5, pp. 75-87.
(16) Durrant, C.J.: 1979, Astron. Astrophys. 73, pp. 137-150.
(17) Glebocki, R., Stawikowski, A.: 1978, Astron. Astrophys. 68, pp. 69-74.
(18) Golub, L., Maxson, C., Rosner, R., Serio, S., Vaiana, G.S.: 1978, Astrophys. J., in press.
(19) Gough, D.O., Weiss, N.O.: 1976, Monthly Not. Roy. Astr. Soc. 176, pp. 589-607.
(20) Habbal, S.R., Leer, E., Holzer, T.E.: 1979, Solar Phys. 64, pp. 287-301.
(21) Hearn, A.G.: 1972, Astron. Astrophys. 19, pp. 417-426.
(22) Hearn, A.G.: 1973, Astron. Astrophys. 23, pp. 97-103.
(23) Hearn, A.G.: 1976, Physique des mouvements dans les atmosphères stellaires, Colloque intern. du CNRS 250, R. Cayrel and M. Steinberg eds., p. 65.
(24) Ionson, J.A.: 1978, Astrophys. J. 226, pp. 650-673.
(25) Kalkofen, W., Ulmschneider, P.: 1979, Astrophys. J. 227, pp. 655-663.
(26) Kelch, W.L., Linsky, J.L., Worden, S.P.: 1979, Astrophys. J. 229, pp. 700-712.
(27) Kotov, V.A., Severny, A.B., Tsap, T.T.: 1979, Solar Oscillations and the Internal Structure of the Sun, Report USSR Academy of Sciences.
(28) Kuperus, M., Ionson, J.A., Spicer, D.F.: 1980, Annual Rev. Astron. Astrophys., in press.
(29) Kurucz, R.L.: 1974, Solar Physics 34, pp. 17-23.
(30) Lamers, H.J.G.L.M., de Loore, C.: 1976, Physique des mouvements dans les atmosphères stellaires, Colloque intern. du CNRS 250, R. Cayrel and M. Steinberg eds., pp. 453-458.
(31) Lighthill, M.J.: 1952, Proc. Roy. Soc. London A 211, pp. 564-587.
(32) Linsky, J.L.: 1980, Proc. of IAU Coll 51, Stellar Turbulence, D.F. Gray, J.L. Linsky eds., Springer, Heidelberg, pp. 248-277.
(33) Linsky, J.L.: 1980, Annual Rev. Astron. Astrophys., in press.
(34) Linsky, J.L., Ayres, T.R.: 1978, Astrophys. J. 220, pp. 619-628.
(35) Praderie, F., Thomas, R.N.: 1976, Solar Phys. 50, pp. 333-342.
(36) Renzini, A., Cacciari, C., Ulmschneider, P., Schmitz, F.: 1977, Astron. Astrophys. 61, pp. 39-45.
(37) Rosner, R., Golub, L., Coppi, B., Vaiana, G.S.: 1978, Astrophys. J. 222, pp. 317-332.

(38) Schmitz, F., Ulmschneider, P.: 1980, Astron. Astrophys., in press.
(39) Somov, B.V., Syrovatskii, S.I.: 1977, Solar Phys. 55, pp. 393-399.
(40) Stein, R.F.: 1968, Astrophys. J. 154, pp. 297-306.
(41) Stein, R.F.: 1980, preprint.
(42) Stein, R.F., Leibacher, J.W.: 1974, Annual Rev. Astron. Astrophys. 12, pp. 407-435.
(43) Stein, R.F., Leibacher, J.W.: 1980, Proc. IAU Coll. 51, Stellar Turbulence, D.F. Gray, J.L. Linsky eds., Springer, Heidelberg, pp. 225-247.
(44) Uchida, Y., Kaburaki, O.: 1974, Solar Phys. 35, pp. 451-466.
(45) Ulmschneider, P.: 1979, Space Sci. Rev. 24, pp. 71-100.
(46) Ulmschneider, P., Schmitz, F., Kalkofen, W., Bohn, H.U.: 1978, Astron. Astophys. 70, pp. 487-500.
(47) Vaiana, G.S. et al.: 1980, preprint.
(48) Vernazza, J.E., Avrett, E.H., Loeser, R.: 1980, Astrophys. J. Suppl., in press.